Nanomed J. 12(2): 252-261, Spring 2025

RESEARCH PAPER

New CuO nanocomposite as non-enzymatic glucose biosensor

Mojtaba Ghorbani [1, 2], Aliakbar Tarlani [1], Saeed Taghvaei-Ganjali [2]*, Mercede Malekzade [2]*

[1]Department of Chemistry, Chemistry & Chemical Engineering Research Center of Iran (CCERCI), Tehran, Iran
[2]Department of Chemistry, Islamic Azad University, North Tehran Branch, Postal Code: 1913674711, Tehran, Iran

ABSTRACT

Objective(s): In a new approach, copper(II) oxide (CuO) nanostructure was synthesized by a solvothermal method for applying as a biosensor for detecting of glucose. Determination of the glucose is important in controlling of diabetes. Non-enzymatic detection of glucose is preferable because of its low cost benefits. Otherwise, CuO can play a role in oxidation of glucose to gluconic acid which is important in glucose detection. Therefore, obtaining new morphology or new composite from CuO is interesting.

Materials and Methods: CuO nanostructure was prepared with the assistance of a bifunctional amino acid of L-lysine (with the isoelectric point about 10 for precipitating copper ion) and an additive of urea. Fourier transform infrared (FT-IR) and Raman spectroscopies, X-ray diffraction (XRD), field emission scanning electron microscopy (FE-SEM), transmission electron microscopy (TEM), cyclic voltammetry analyses and differential pulse voltammetry (DPV) were employed.

Results: XRD indicated that the synthesized CuO consists of a tenorite crystal system with a monoclinic structure. The TEM histogram showed a mean diameter of 91 nm for CuO nanostructure. CuO nanostructure loaded on graphene oxide-grafted Lisdexamfetamine Dimesylate (LIS) to achieve CuO/LIS-g-GO composite. CuO/LIS-g-GO was dropped on a glassy carbon electrode (GCE) to develop a new nanobiosensor for detecting glucose in a cost-effective manner without the necessity of using glucose oxidase or nafion. Phosphate buffer (PBS) and simulated body fluid (SBF) solutions were the media of the glucose detection. The sensitivity of the biosensor was 34.7 μA/cm^{2}mM for 10 mM concentration of the glucose. The mentioned sensor detected no interference in the presence of dopamine and fructose. Also, the repeatability of the biosensor was investigated and the measured standard deviation (RSD) was 3.93%.

Conclusion: New nanostructured CuO was composited with LIS-g-GO and the new biosensor of CuO/LIS-g-GO/GCE was applied for the detection of glucose. The sensitivity of 34.7 μA/cm^{2}mM without any interference of dopamine and fructose caused this system as favorite sensor for the detection of glucose.

Keywords: *Biosensing technique, Glucose, Lysine, Graphene oxide, Lisdexamfetamine dimesylate, Non-enzymatic*

How to cite this article
Ghorbani M, Tarlani AK, Taghvaei-Ganjali S, Malekzade M. New CuO nanocomposite as non-enzymatic glucose biosensor. Nanomed J. 2025; 12(2): 252-261. DOI: 10.22038/nmj.2024.79481.1962

INTRODUCTION

Diabetes is a serious medical disorder distinguished by chronically high levels of glucose in the blood. The measurement of glucose is crucial for recognizing and controlling diabetes [1]. In order to accomplish the aforementioned goal, several glucose sensors have been designed with different kinds of transducers [2]. Electrochemical glucose sensors have attracted considerable attention because of their affordability, sensitivity, and accessibility. They are categorized as either enzymatic or non-enzymatic. The enzymatic sensors exhibit exceptional selectivity and sensitivity. However, they also experience major drawbacks, including limited durability, chemical instability, hard storage necessities and manufacturing complexity [3]. To tackle all of these problems, significant efforts have been made towards developing appropriate non-enzymatic sensors. Currently, researchers are drawn to graphene because of its greater specific surface area, purity, excellent conductivity and inexpensive cost [4, 5]. Graphene offers a wide range of applications in several fields, including batteries [6], supercapacitors [7], printable electronics [8], gas sensors [9], biosensors [10] and biomedicines [11, 12]. Therefore, it is essential to use environmentally acceptable techniques to

* *Corresponding authors: Emails: Taghvaei@hotmail.com; Tarlani@ccerci.ac.ir*
Note. This manuscript was submitted on April 22, 2024; approved on July 7, 2024

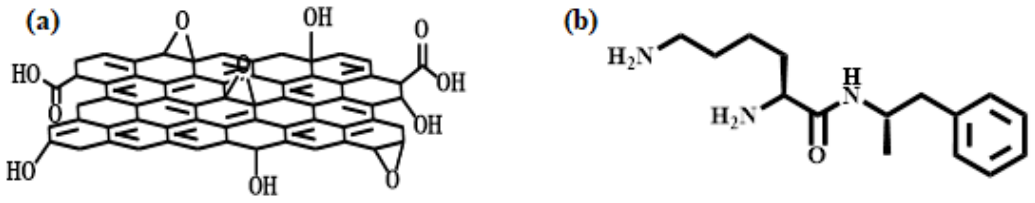

Scheme 1. Structures of GO (a) and LIS (b)

functionalize graphene oxide (GO) for biosensing purposes. The electrocatalytical capability of CuO makes it suitable for functionalizing GO as a catalyst [13]. CuO is a p-type semiconductor that is consistently superior to other materials in the field of nonenzymatic glucose sensing. This property may be ascribed to the favorable electrochemical activity and the capacity to facilitate electron transfer processes [14]. Song et al. presented a glucose biosensor that utilizes CuO nanoparticles (CuONPs) supported on GO nanosheet. The biosensor has a broad linear range spanning from 2.79 µM to 2.03 mM and the limit of detection (LOD) was 0.69 µM while the detecting potential was set at 0.7 V. The CuONPs/GO sensor exhibited a comparable wide linear range of 2.55 µM to 0.5 mM. The sensor exhibited a high degree of selectivity for glucose over interfering substances such as ascorbic acid (AA) and uric acid (UA). Additionally, it demonstrated excellent durability at ambient temperature, with just a 12.5% loss in sensitivity seen after 4 weeks [15]. Alizadeh et al. prepared a glucose biosensor by combining metal oxide with graphene, without using enzymes. The CuO/graphene composite exhibited a low LOD of 0.09 µM. The enhanced capacity to transmit charges, resulting from the combination of CuO and graphene sheet, is considered to be the main factor behind the superior performance of the glucose sensor [16]. Li et al. fabricated a non-enzymatic glucose sensor by producing graphene-CuO nanocomposites and attaching them to a GCE using Nafion. The mentioned glucose biosensor showed a linear range from 2.0 µM to 0.06 mM and a minimal detection limit of 0.29 µM (S/N = 3). The interference of AA, dopamine (DA), and UA was not observed [17]. Nafion has significant drawbacks including high cost, limited performance at temperatures over 80 °C, and the potential to release environmentally persistent and hazardous substances. Materials based on GO have the potential to serve as an alternative to Nafion [18]. The conductivity, stability, and selectivity of GO are enhanced by functionalization, leading to improved performance in electrochemical sensing applications. Additionally, increasing the graphene oxide surface area raises its sensitivity [19-21]. Lisdexamfetamine Dimesylate (LIS) is a compound that is converted into dextroamphetamine, a kind of stimulant that affects the central nervous system [22]. This conversion usually occurs by attaching dextroamphetamine to the amino acid L-lysine, which is naturally found in the body [23].

This work involves the solvothermal synthesis of CuO nanostructure using a novel additive. Usually, GO was modified the biosensors while in this report, new composite from graphene oxide was synthesized, characterized, and applied for biosensing of the glucose. This nanostructure is subsequently used to detect glucose biomolecule using a non-enzymatic method. The investigation used a cost-effective and bare GCE that was enhanced using graphene oxide grafted LIS. The chemical structures of GO and LIS are depicted in Scheme 1.

MATERIALS AND METHODS

Graphite powder, measuring less than 70 µm in diameter, was obtained from Shimi Pajohesh Asia Co. Copper(II) nitrate trihydrate, lysine, urea, potassium hydroxide, and ethanol were purchased from Merck Chemical Co. Dopamine hydrochloride and fructose were purchased from Sigma Aldrich. LIS was gifted from Tadbir Kalaye Jam Co. (Tekaje).

The FT-IR spectra of graphene oxide and its composite were acquired using a Fourier transform infrared spectrometer, Spectrum 65 (PERKIN-ELMER). The spectra were obtained with a resolution of 4 cm^{-1}, and the scanning was performed in the wavenumber range of 400–4000 cm^{-1}. The Raman spectra of graphene oxide and its composite were performed on TESCAN (model TakRam N1-541, Iran). XRD was utilized to determine the crystal structure of both graphene oxide and the recently changed graphene. The XRD patterns were acquired with a powder X-ray

diffractometer, the Bruker AXS-D8 Advance. The device was fitted with a copper target and functioned at a wavelength of λ CuKa = 1.54056 Å. The voltage and current applied to the tube were adjusted to 40 kV and 30 mA, respectively. The XRD patterns were obtained within the angular range of 5° to 80°, using a scanning speed of 0.05°/s. The structure of graphene oxide and other drug-modified graphene oxide was analyzed using a field emission scanning electron microscope (FE-SEM) produced by TESCAN (model MIRA III, Czech Republic). The electrochemical analysis was conducted using a potentiostat/Galvano stat μAutolab type III (Metrohm Auto lab).

Synthesis of graphene oxide

At first, a glass container wa placed into a chilled bath. During the first stage of this experimental phase, it was crucial to maintain a temperature below 10 oC by submerging the thermometer in the bath. 46 mL of sulfuric acid with a concentration of 98% was added to the container, then 2 g of pure graphite added. The contents of the container were then agitated for duration of 15 min. 6 g of potassium permanganate powder was added slowly to the mixture while aggressively agitated for 1.5 hr. After completing the mixing step, the stirring was continued for an extra 0.5 h. Subsequently, the bath temperature was raised to 35 °C. After reaching to a stable temperature, the mixing process was continued for an additional hour. To accomplish dilution, 400 mL of distilled water was added to the container, and then the mixture was continuously stirred for 30 min. It is crucial to maintain the bath temperature below 40 °C at this point. After adding distilled water to the mixture, 20 mL of hydrogen peroxide with a concentration of 30% was slowly added to the container. The mixing operation was continued for a period of 0.5 hr. During this specific stage, the solution experiences a short transition, leading to a change in color to a light-yellow. Afterwards, the mixture underwent a washing procedure including a 1 M hydrochloric acid solution, followed by a further rinse with distilled water. The objective of this process was to remove ions and increase the pH level [24].

Synthesis of functionalized graphene oxide

The addition of 100 mg of graphene oxide to 200 mL of deionized water in a 500 mL round-bottom flask resulted in the formation of a uniform dispersion. Afterwards, a solution containing 200 mg of LIS and 200 mg of potassium hydroxide was added and exposed to ultrasonic instrument for 1 h. Subsequently, the mixture was moved to an oil bath and exposed to reflux at a temperature of 80 °C for a period of 24 hr, with constant stirring until a homogeneous black solution was obtained. The solution was filtered using a nanofilter system, then washed with a 1 M hydrochloric acid solution, and finally rinsed with distilled water. The collected sediment was put cautiously into a beaker and then placed into a desiccator equipped with a vacuum valve at a consistent ambient temperature [25].

Synthesis of CuO

Initially, 2.04 g of urea and 0.58 g of lysine were introduced into the beaker. Subsequently, a 40 mL solution consisting equal parts of water and ethanol added to the beaker and mixed thoroughly. A quantity of 3.09 g of copper(II) nitrate was introduced into a separate container, followed by the addition and complete mixing of 40 mL water and ethanol solution. The contents of two beakers were combined in a 200-mL beaker and agitated for 15 min using a magnetic stirrer. The pH of the mixture was determined between 2 and 3. The solution obtained was subjected to a heating process for duration of 20 h at a temperature of 150 °C using a Teflon lined autoclave. The resulting product was cooled, and its pH was determined to be 9. Subsequently, it was filtered and subjected to drying in an oven at a temperature of 50 °C. The sediment was pulverized in a mortar to achieve a consistent particle size. The process of calcination carried out at a temperature of 600 °C, with a heating rate of 5 °C/min for duration of 3 hr inside the furnace.

Loading of CuO on LIS-*g*-GO

In the beginning, CuO was dissolved in a 10 mL solution of diethylene glycol. Subsequently, the functionalized graphene oxide was introduced, followed by the addition of 10 mL deionized water. The sample underwent ultrasonication for duration of 30 min. Subsequently, the mixture was agitated using a magnetic stirrer operating at a speed of 200 rpm at a temperature of 80 °C for duration of 20 hr. This process took place inside a glass container, which was sealed with an aluminum foil cover. Afterward, the mixture was subjected to centrifugation and subsequently

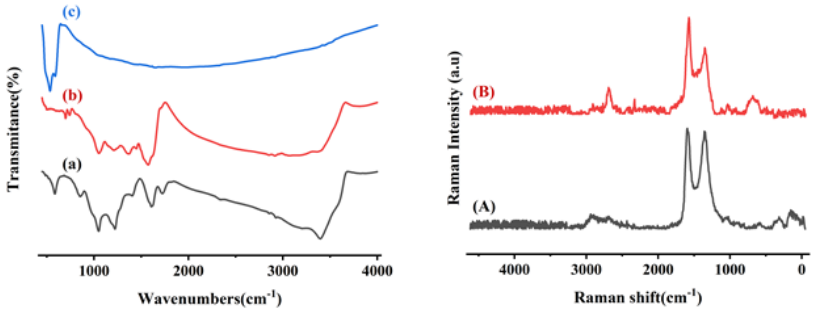

Fig. 1. FT-IR & Raman spectra of GO (a,A), LIS-g-GO (b,B), and CuO (c)

separated. It underwent multiple washes with water and ethanol before being subjected to drying in an oven at a temperature of 50 °C. A quantity of 5 mg of the dehydrated mixture was evenly distributed in 5 mL of dimethylformamide using ultrasonic vibrations for duration of 1 hr. Subsequently, it was agitated within a container for 24 hr. A volume of 3 µL of the suspension dropped onto the electrode using a sampler and then desiccated in an oven. Following that, the electrode containing desiccated powder was employed to quantify the prepared solutions by varying concentrations utilizing the auto-lab device [26, 27].

RESULTS AND DISCUSSIONS

FT-IR analysis & Raman spectroscopy

Fig. 1(a-c) displays the FT-IR spectra of GO, LIS-g-GO, and CuO. The absorption peak 3396 cm^{-1} is ascribed to the stretching vibration of the O-H bonds present in carboxylic acid and the hydroxyl groups of GO. The vibrational mode at 1725 cm^{-1} corresponds to the stretching of C=O bonds in carboxylic acid groups inside GO. The presence of a C=C strong vibrational peak at 1607 cm^{-1} implies the formation of hexagonal structure of GO and graphene. Following functionalization with amino biomolecules, the strength of the C=O stretching mode decreases. Instead, a new vibrational mode associated with the stretching of C=O bonds in amide groups appears at a lower wavelength of 1622 cm^{-1}. The presence of OH and NH stretching bands about 3400 cm^{-1} provides evidence for the formation of nanocomposites between GO and amino biomolecules. The presence of peaks at 1049 and 852 cm^{-1} indicates the occurrence of C-O stretching related to epoxy groups. The presence of a doublet peak at 2850 and 2915 cm^{-1} in the infrared spectrum indicates the existence of symmetric and asymmetric CH_2 in the alkyl moieties of GO (Fig. 1a) [28]. The FT-IR spectra of LIS-g-GO demonstrated the presence of the C–N bond at a wavenumber of 1365 cm^{-1} [29] (Fig. 1b). The peak at 588 and 534 cm^{-1} confirms the metal oxygen bond (Cu–O) [30] (Fig. 1c).

Fig. 1(A-B) shows the Raman spectra of GO and LIS-g-GO, respectively. The use of Raman spectroscopy was employed to assess both the quality and structural characteristics of GO and functionalized GO. The alterations were seen in the primary features such as D, G, and 2D bands which are indicative of the functionalization process undergone by GO [31]. The GO and LIS-g-GO samples exhibited characteristic G and D bands at wavenumbers of 1594 & 1357 cm^{-1} and 1572 & 1351 cm^{-1}, respectively. The sp3/sp2 carbon ratio (ID/IG) of GO and LIS-g-GO is 0.97 and 0.69, respectively. The LIS-g-GO sample, with an ID/IG ratio of 0.69, demonstrated a higher degree of the graphite phase [32, 33].

XRD studies

In Fig. 2, the XRD pattern was compared with the standard JCPDS file number 96–901-5823. The marked (110), (002), (11-1), (111), (200), (20-2), (020), (202), (11-3), (31-1), and (220) diffraction peaks in the XRD pattern are well matched with the aforementioned standard JCPDS file number which the (11-1) and (111) peaks have the highest

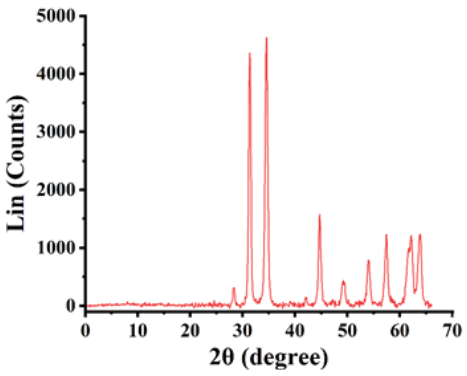

Fig. 2. XRD pattern of CuO

intensity in comparison with other peaks. According to the data, the formed CuO nanostructure consists of a tenorite crystal system in a single-phase with a monoclinic structure (space group C 1 2/c 1). Lattice parameters are a = 4.67 Å, b = 3.45 Å, and c = 5.12 Å, respectively [34, 35].

Morphological studies

FE-SEM was used to confirm the morphologies and feature sizes of the samples and to confirm that LIS-g-GO and CuO were made successfully in the reaction mixture, as shown in Fig. 3(a-f). Stacked flakes are a prevalent kind of functionalized nanostructure [36]. The surface morphology of GO analyzed using SEM that revealed sheet-like morphology before grafting with LIS (Fig. 3(a-b)), whereas the composite showed aggregated morphology, which could be due to the presence of amino biocompound (Fig. 3(c-d)) [37]. From the Fig. 3(e-f), it is clearly seen that the CuO particles are spherical in shape. The surface is not smoother. But the particle size lies well within nano range [38].

The TEM micrographs of LIS-g-GO and CuO are shown in Fig. 4 (a-b, c-d), respectively. Black areas represent dense packing of the GO layers and the presence of oxygen functional groups, while the transparent areas show the exfoliated stacking nanostructure of thinner GO layers [39].

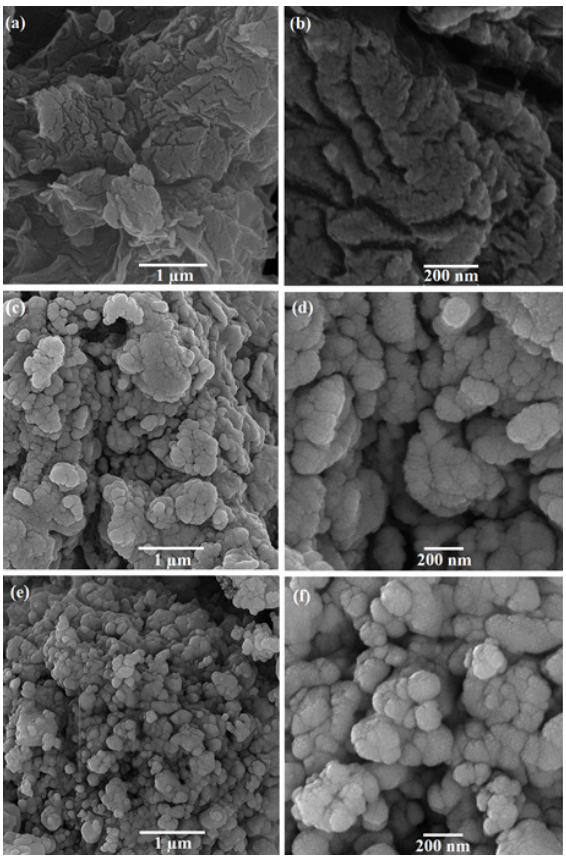

Fig. 3. FE-SEM micrographs of GO (a,b), LIS-g-GO (c,d), and CuO (e,f)

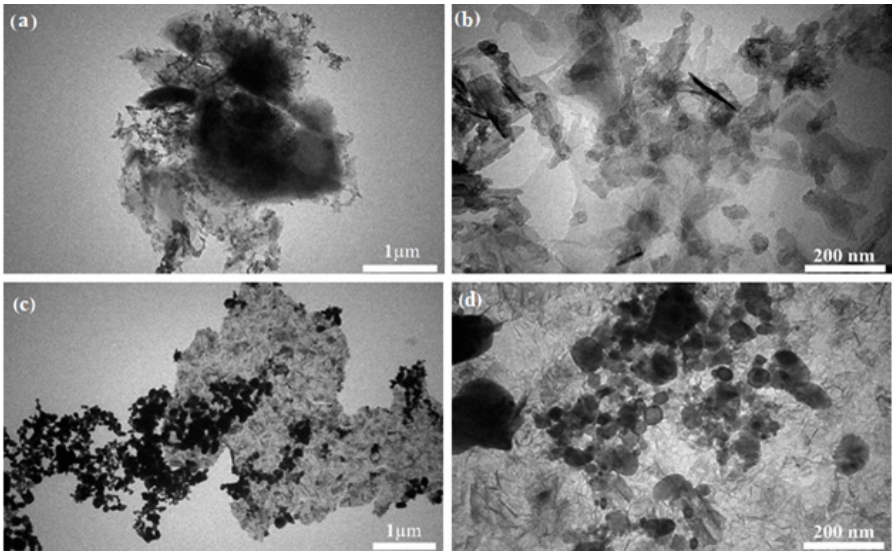

Fig. 4. TEM micrographs of LIS-g-GO (a,b) and CuO (c,d)

The histograms depicting the distribution of particle sizes, as calculated from the micrographs obtained using TEM, revealed a significant degree of variance in particle size. The particle sizes of LIS-g-GO and CuO fall within the range of 70–110 nm. The mean diameters of LIS-g-GO and CuO are 89 and 91 nm, respectively. The histograms in Fig. 5(a–b) depict the particle size distribution of LIS-g-GO and CuO, respectively.

Repeatability, interference, and stability studies

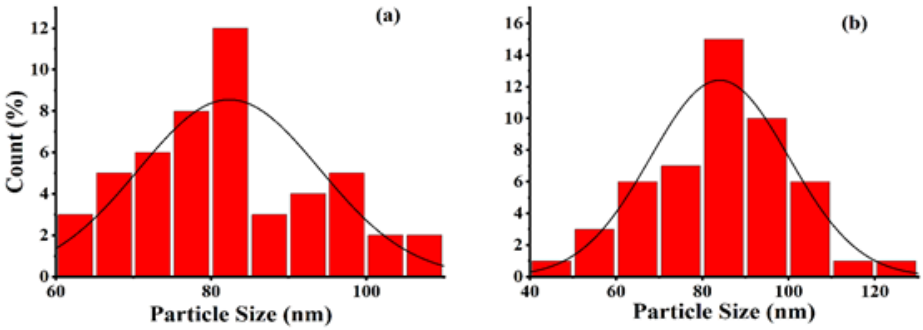

Fig. 5. Particle size distribution histograms of LIS-g-GO (a) and CuO (b)

of biosensor

Fig. 6 shows CV of bare GCE in PBS, CuO/LIS-g-GO/GCE in PBS, and CuO/LIS-g-GO/GCE in 10 mM glucose. The best response was related to 10 mM concentration of glucose solution with sensitivity of 34.7 µA/cm2mM [40].

To essay the repeatability of the biosensor, CuO/LIS-g-GO/GCE was repetitively applied for measuring 10 mM of glucose concentration for three times. The measured RSD was 3.93%. To verify the sensitivity of the CuO/LIS-g-GO/GCE biosensor as a function of glucose concentrations, 2, 4, 6, 8, 10, 12, and 14 mM glucose solutions were prepared for biosensing at room temperature, Fig. 7(a). Calibration curve of the biosensor with the correlation coefficient of 0.9018 is depicted in Fig. 7(b). The detection limit of the biosensor was 1.16 mM. The quantitation limit of the biosensor was 3.86 mM. As can be seen, enhancement of the current response observed while the concentration of glucose was increased. Furthermore, the electrochemical response of interfering DA and fructose (Fr) at the concentration of 0.4 mM was studied for the CuO/LIS-g-GO/GCE biosensor in PBS, Fig. 7(c). Results revealed that DA and Fr do not show the response in the presence of 4 mM of glucose [41]. The biosensor was stored at room temperature for two weeks and the stability of the sensor was checked. No significant reduction in biosensor performance was observed when measuring 8 mM glucose solution. The performance of the biosensor is illustrated by the recovery values for accuracy and the coefficient of variation for precision, which are presented in Table 1.

DPV measurement was performed to examine the influence of glucose concentration. DPV measurement is considered as a suitable technique which can minimize the effects of capacitive currents that occur during glucose oxidation. Therefore, the measured current is a pure Faradaic current resulting from the influence of glucose concentration. DPV measurement was performed by changing glucose concentration from 2-14 mM in PBS solution. The DPV current increased with increasing glucose concentration. The findings

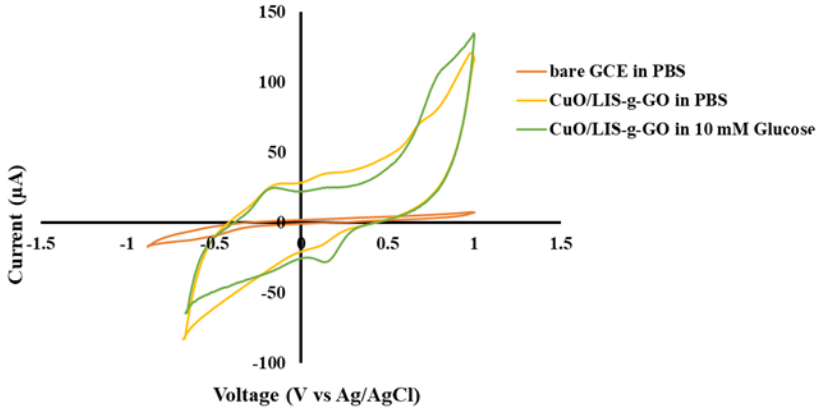

Fig. 6. CV of bare GCE in PBS, CuO/LIS-g-GO/GCE in PBS, and CuO/LIS-g-GO/GCE in 10 mM glucose

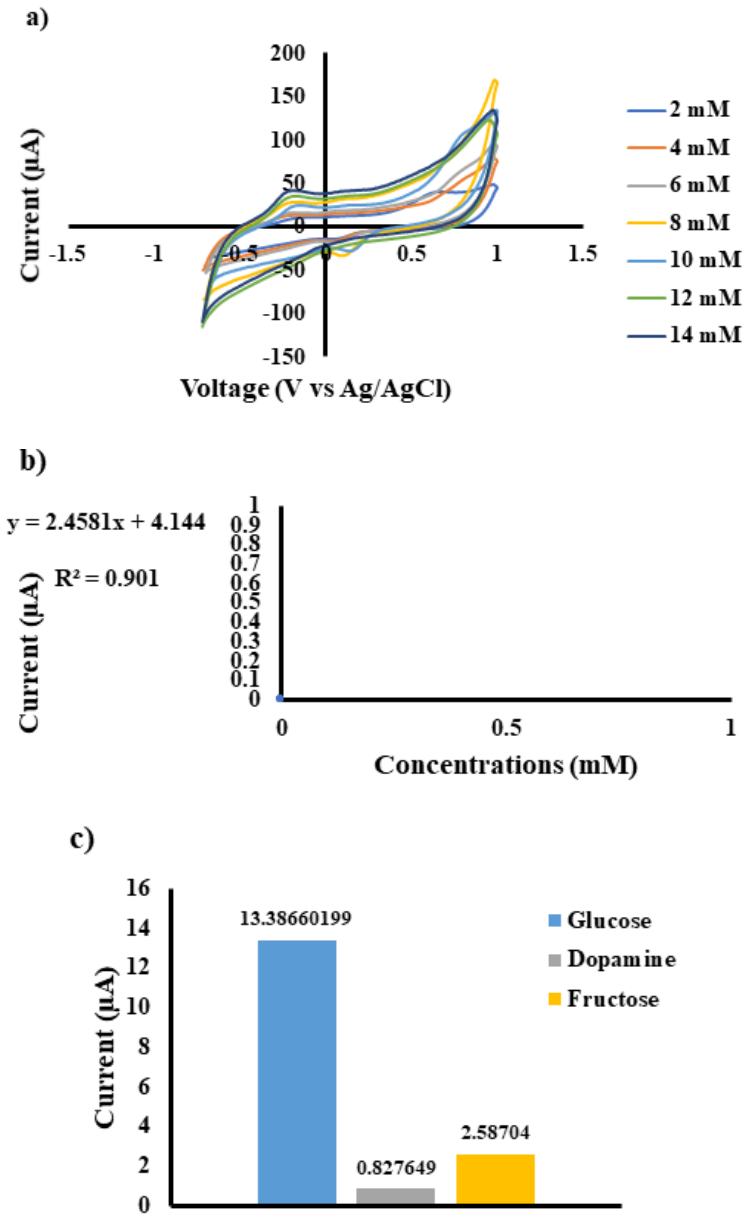

Fig. 7. CuO/LIS-g-GO/GCE applied in (a) plotting CV of changing glucose concentration from 2 to 14 mM in PBS, (b) Calibration curve of the biosensor (c) interference test with 4 mM glucose and other electroactive species including 0.4 mM DA and 0.4 mM Fr in PBS

Table 1. Accuracy and precision of the biosensor

Glucose added (mM)	Glucose calculated (mM)	% Recovery	Coefficient of variation
6	5.7	95	0.026
8	8.3	103.75	0.018

are displayed in Fig. 8a. Fig. 8b shows the linear regression plot between the values of the current and the values of the glucose concentration.

Real sample analysis

The CuO/LIS-g-GO/GCE biosensor was employed in the detection of glucose in simulated body fluid (SBF). To accomplish this, SBF was chosen as the medium for glucose measurement [42, 43]. The result exhibited that the biosensor showed a dose dependence response. Also, it confirmed that, biosensing of the glucose by means of CuO/LIS-g-GO/GCE electrode is feasible without any interference. This is an advantage for this electrode that without using nafion or glucose oxidase, glucose is detectable in the presence of electroactive species. Therefore, it could be concluded that, simple and low cost CuO/LIS-g-GO/GCE biosensor can sense the glucose efficiently and selectively. Different amounts of glucose with 5 mM concentration were spiked into the SBF. For cyclic voltammetry, a potential window from −1 V to +1 V was operated with a scan rate of 0.1 mV/s. The CV of different standards is shown in Fig. 9. The recovered concentration and recovery (%) of the spiked samples using the biosensor were 8.82 mM and 56.69%, respectively.

Table 2 provides a summary of several nano biosensors for Glucose detection.

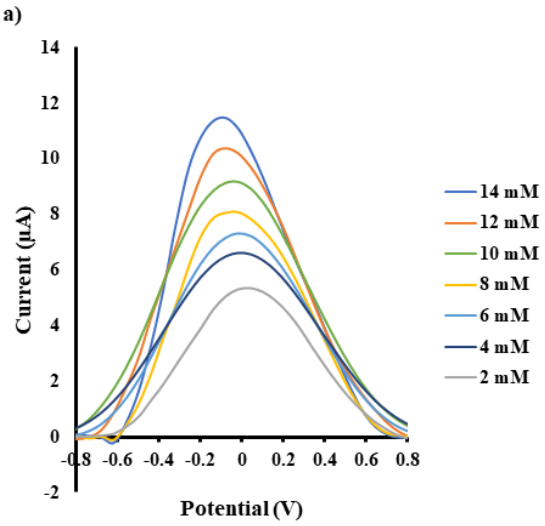

Fig. 8. (a) DPV measurement of glucose in 0.01 M of PBS pH 7.4 with the variation concentration of (2–14 mM); (b) Linear regression plot between the values of the current and the values of the glucose concentration

CONCLUSION

CuO crystalline nanostructure was synthesised via a solvothermal by interaction of copper(II) nitrate, lysine amino acid and urea (as precipitating and directing agents). On the other hand, Graphene oxide was grafted with LIS to achieve LIS-g-GO. Finally, the prepared nanostructure and CuO/LIS-g-GO was loaded on glassy carbon electrode (GCE) to obtain CuO/LIS-g-GO/GCE nano biosensor to detect glucose. CuO/LIS-g-GO/GCE

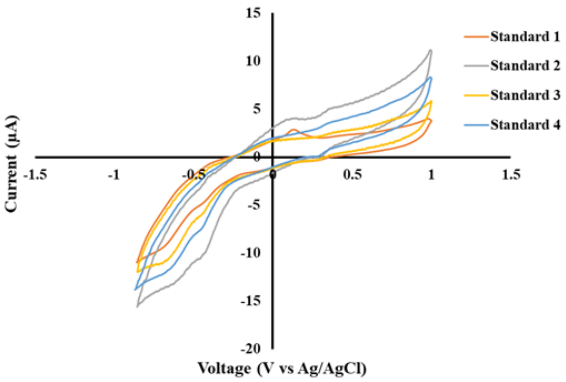

Fig. 9. CuO/LIS-g-GO/GCE applied in plotting CV of different amounts of glucose with 5 mM concentration spiked into the SBF

Table 2. Comparison of different nano biosensors for Glucose detection

Electrode matrix	Enzymatic/ nonenzymatic	Sensitivity	Detection limit (mM)	References
CuO/LIS-g-GO	nonenzymatic	34.7	1.16	This work
Cu_2O/graphene nanosheet	nonenzymatic	-	1.2	[44]
CuO/graphene	nonenzymatic	-	6.7 × 1	[45]
Cu_2O/graphene nanosheets	nonenzymatic	-	3.3	[46]
Cu_2O/rGO	nonenzymatic	19.5 µA/mM^{-1}	-	[47]
Cu_2O/NiOx/GO	enzymatic	-	-	[48]

biosensor was used for sensing in PBS and SBF. The sensitivity of the biosensor was 34.7 µA/cm2 mM. The CuO/LIS-g-GO/GCE biosensor was tested in different concentrations (2-14 mM) of glucose and the interference effect was investigated in the presence of DA and Fr (0.4 mM). The DPV current increased with increasing glucose concentration.

ACKNOWLEDGEMENTS

We express our gratitude to the Chemistry & Chemical Engineering Research Center of Iran (CCERCI) for their kind assistance. Authors would like to thank Dr. Farnoush Faridbod from University of Tehran for her assistance in sensor tests. No funding was received for conducting this study.

CONFLICTS OF INTEREST

There is no conflict of interest to mention.

REFERENCES

1.1. Lee H, Choi TK, Lee YB, Cho HR, Ghaffari R, Wang L, et al. A graphene-based electrochemical device with thermoresponsive microneedles for diabetes monitoring and therapy. Nat Nanotechnol. 2016;11(6): 566-572.
2. Niu X, Li X, Pan J, He Y, Qiu F, Yan Y. Recent advances in non-enzymatic electrochemical glucose sensors based on non-precious transition metal materials: opportunities and challenges. RSC Adv. 2016;6(88): 84893-84905.
3. Fan Z, Liu B, Liu X, Li Z, Wang H, Yang S, et al. A flexible and disposable hybrid electrode based on Cu nanowires modified graphene transparent electrode for non-enzymatic glucose sensor. Electrochim. Acta. 2013;109: 602-608.
4. Liu F, Wang C, Sui X, Riaz MA, Xu M, Wei L, et al. Synthesis of graphene materials by electrochemical exfoliation: Recent progress and future potential. Carbon Energ. 2019;1(2):173-199.
5. Oorimi PG, Tarlani A, Zadmard R, Muzart J. Synthesis of photoluminescent composite based on graphene quantum dot@ ZIF-11: A novel sensor for extremely efficient nano-molar detection of CN–. Microchem J. 2023;189:108494-109502.
6. Ji L, Meduri P, Agubra V, Xiao X, Alcoutlabi M. Graphene-based nanocomposites for energy storage. Adv Energy Mat. 2016;6(16):1502159 (1-73).
7. Hota P, Miah M, Bose S, Dinda D, Ghorai UK, Su Y-K, et al. Ultra-small amorphous MoS2 decorated reduced graphene oxide for supercapacitor application. J Mat Sci Technol. 2020;40:196-203.
8. Hu A, Li R, Bridges D, Zhou W, Bai S, Ma D, et al. Photonic nanomanufacturing of high performance energy devices on flexible substrates. J Laser Appl. 2016;28(2) 022602 (1-4).
9. Nakate UT, Choudhury SP, Ahmad R, Patil P, Nakate YT, Hahn Y-B. Graphene oxide (GO) nanocomposite based room temperature gas sensor. Func. Nanomat.: Adv Gas Sens Technol. 2020:303-328.
10. Bai Y, Xu T, Zhang X. Graphene-based biosensors for detection of biomarkers. Micromachines. 2020;11(1):60 (1-19).
11. Mallick A, Mahapatra A, Mitra A, Greneche J-M, Ningthoujam R, Chakrabarti P. Magnetic properties and bio-medical applications in hyperthermia of lithium zinc ferrite nanoparticles integrated with reduced graphene oxide. Journal of Applied Physics. 2018;123(5) 055103 (1-9).
12. Ghorbani M, Tarlani A, Taghvaei-Ganjali S, Malekzade M. Nanostructures Originated from Grafting Amino Group Containing Biomolecules on Graphene Oxide. ChemistrySelect. 2024;9(16):e202304045 (1-16).
13. Khan M, Nagal V, Nakate UT, Khan MR, Khosla A, Ahmad R. Engineered CuO nanofibers with boosted non-enzymatic glucose sensing performance. J Electrochem Soc. 2021;168(6):067507 (1-8).
14. Meher SK, Rao GR. Archetypal sandwich-structured CuO for high performance non-enzymatic sensing of glucose. Nanoscale. 2013;5(5):2089-2099.
15. Song J, Xu L, Zhou C, Xing R, Dai Q, Liu D, et al. Synthesis of graphene oxide based CuO nanoparticles composite electrode for highly enhanced nonenzymatic glucose detection. ACS Applied Mat. Interfaces. 2013;5(24):12928-12934.
16. Alizadeh T, Mirzagholipur S. A Nafion-free non-enzymatic amperometric glucose sensor based on copper oxide nanoparticles–graphene nanocomposite. Sens. Actuators B: Chem. 2014;198:438-447.
17. Li Y, Huang F, Chen J, Mo T, Li S, Wang F, et al. A high performance enzyme-free glucose sensor based on the graphene-CuO nanocomposites. Int J Electrochem Sci. 2013;8(5):6332-6342.
18. Di Virgilio M, Basso Peressut A, Arosio V, Arrigoni A, Latorrata S, Dotelli G. Functional and environmental performances of novel electrolytic membranes for PEM fuel cells: a lab-scale case study. Clean Technol. 2023;5(1):74-93.
19. Shams N, Lim HN, Hajian R, Yusof NA, Abdullah J, Sulaiman Y, et al. Electrochemical sensor based on gold nanoparticles/ethylenediamine-reduced graphene oxide for trace determination of fenitrothion in water. RSC Adv. 2016;6(92):89430-89439.
20. Singh RK, Kumar R, Singh DP. Graphene oxide: strategies for synthesis, reduction and frontier applications. Rsc Adv. 2016;6(69):64993-65011.
21. Chen D, Feng H, Li J. Graphene oxide: preparation, functionalization, and electrochemical applications. Chem Rev. 2012;112(11):6027-6053.
22. Goodman DW. Lisdexamfetamine dimesylate (vyvanse), a prodrug stimulant for attention-deficit/hyperactivity disorder. Pharm Therapeutics. 2010;35(5):273-287.
23. Madaan V. Lisdexamfetamine dimesylate for childhood ADHD. Drugs of Today (Barcelona, Spain: 1998). 2008;44(5):319-324.
24. Hummers Jr WS, Offeman RE. Preparation of graphitic oxide. J Am Chem Soc. 1958;80(6):1339-1339.
25. Yang J, Liu C, Gao L, Wang J, Xu Y, He R. Novel composite membranes of triazole modified graphene oxide and polybenzimidazole for high temperature polymer electrolyte membrane fuel cell applications. Rsc Adv. 2015;5(122):101049-101054.
26. Tarlani A, Fallah M, Lotfi B, Khazraei A, Golsanamlou S, Muzart J, et al. New ZnO nanostructures as non-enzymatic glucose biosensors. Biosens Bioelectron. 2015;67:601-607.
27. Khazraei A, Tarlani A, Eslami-Moghadam M, Muzart J. New Bi2MoO6 nano-shapes toward ultrasensitive enzymeless glucose tracing: Synergetic effect of the Bi-Mo association. Talanta. 2021;221:121560 (1-10).

28. Surekha G, Krishnaiah KV, Ravi N, Suvarna RP. FTIR, Raman and XRD analysis of graphene oxide films prepared by modified Hummers method. J Phys: Conf Ser; 2020: IOP Publishing.1495 (2020) 012012 (1-6).
29. M Hashem H, SM Hassan S, H Kamel A, Amr AE-GE, AbdelBary E. Cost-Effective Potentiometric Platforms Modified with Multi-Walled Carbon Nanotubes (MWCNTs) and Based on Imprinted Receptors for Fluvoxamine Assessment. Polymers. 2020;12(3):673 (1-14).
30. Mahalingam S, Ramasamy J, Ahn Y-H. Enhanced photocatalytic degradation of synthetic dyes and industrial dye wastewater by hydrothermally synthesized G–CuO–Co 3 O 4 hybrid nanocomposites under visible light irradiation. J Cluster Sc. 2018;29:235-250.
31. Vecera P, Chacón-Torres JC, Pichler T, Reich S, Soni HR, Görling A, et al. RETRACTED ARTICLE: Precise determination of graphene functionalization by in situ Raman spectroscopy. Nat Commun. 2017;8(1):15192 (1-9).
32. Georgakilas V. Covalent attachment of organic functional groups on pristine graphene. Funct. Graphene C. 2014:21-58.
33. Qiao S-J, Xu X-N, Qiu Y, Xiao H-C, Zhu Y-F. Simultaneous reduction and functionalization of graphene oxide by 4-hydrazinobenzenesulfonic acid for polymer nanocomposites. Nanomater. 2016;6(2):29 (1-10).
34. Calos N, Forrester J, Schaffer G. A crystallographic contribution to the mechanism of a mechanically induced solid state reaction. J Solid State Chem. 1996;122(2):273-280.
35. Fatima B, Siddiqui SI, Ahmad R, Linh NTT, Thai VN. CuO-ZnO-CdWO4: a sustainable and environmentally benign photocatalytic system for water cleansing. Environ Sci Pollut Res. 2021;28(38):53793-53803.
36. Zarafu I, Turcu I, Culiță DC, Petrescu S, Popa M, Chifiriuc MC, et al. Antimicrobial features of organic functionalized graphene-oxide with selected amines. Mater. 2018;11(9):1704 (1-10).
37. Pravin M, Gnanamani A. Preparation, characterization and reusability efficacy of amine-functionalized graphene oxide-polyphenol oxidase complex for removal of phenol from aqueous phase. RSC Adv. 2018;8(67):38416-38424.
38. Rout S. Synthesis and Characterization of CuO/graphene oxide composite 2013 (1-25).
39. Stobinski L, Lesiak B, Malolepszy A, Mazurkiewicz M, Mierzwa B, Zemek J, et al. Graphene oxide and reduced graphene oxide studied by the XRD, TEM and electron spectroscopy methods. J Electron Spectros Relat Phenomena. 2014;195:145-154.
40. Zang J, Li CM, Cui X, Wang J, Sun X, Dong H, et al. Tailoring zinc oxide nanowires for high performance amperometric glucose sensor. Electroanalysis: An Int J Devoted Fundament. Pract Asp Electroanal. 2007;19(9):1008-1014.
41. Liu S, Yu B, Zhang T. A novel non-enzymatic glucose sensor based on NiO hollow spheres. Electrochim Acta. 2013;102:104-107.
42. Kiani M, Tehrani MA, Sayahi H. Reusable and robust high sensitive non-enzymatic glucose sensor based on Ni (OH)2 nanoparticles. Anal Chim Acta. 2014;839:26-33.
43. Xu W, Gao Q, Xu Y, Wu D, Sun Y, Shen W, et al. Controllable release of ibuprofen from size-adjustable and surface hydrophobic mesoporous silica spheres. Powd. Technol. 2009;191(1-2):13-20.
44. Qian Y, Ye F, Xu J, Le Z-G. Synthesis of cuprous oxide (Cu2O) nanoparticles/graphene composite with an excellent electrocatalytic activity towards glucose. Int J Electrochem Sci. 2012;7(10):10063-10073.
45. Yu H-Y, Xu M-Q, Yu S-H, Zhao G-C. A novel non-enzymatic glucose sensor based on CuO-graphene nanocomposites. Int J Electrochem Sci. 2013;8(6):8050-8057.
46. Liu M, Liu R, Chen W. Graphene wrapped Cu2O nanocubes: non-enzymatic electrochemical sensors for the detection of glucose and hydrogen peroxide with enhanced stability. Biosens. Bioelectron. 2013;45:206-212.
47. Xu F, Deng M, Li G, Chen S, Wang L. Electrochemical behavior of cuprous oxide–reduced graphene oxide nanocomposites and their application in nonenzymatic hydrogen peroxide sensing. Electrochim. Acta. 2013;88:59-65.
48. Yuan B, Xu C, Liu L, Zhang Q, Ji S, Pi L, et al. Cu2O/NiOx/graphene oxide modified glassy carbon electrode for the enhanced electrochemical oxidation of reduced glutathione and nonenzyme glucose sensor. Electrochim. Acta. 2013;104:78-83.